Designing and Simulation of Double Stage Grid-Linked PV System Using MATLAB/Simulink

Shamik Kumar Das, M. K. Sinha, and A. K. Prasad

1 Introduction

It has been seen that the production and consumption rates of fossil fuels have increased exponentially in the last decade worldwide. It has been predicted that the coal reserves of India will last for 200 years only, and crude oil will run out in the next 25 years at the current consumption rate. Importing conventional sources of energy is not a healthy option to sustain the energy security of a country. So, we have to invest, promote, and utilize renewable sources as an alternative to conventional sources to meet the energy demand with fewer environmental hazards and to decrease the import dependency as well as the alignment toward fossil fuels.

Among the non-conventional energy applications, photovoltaic technology is one of the important applications to generate electricity using solar energy due to its fastest-growing PV technology, no fuel cost, less installation space, lack of noise, and low maintenance cost. Overall, solar energy is an inexhaustible, pollution-free, and clean source of energy. However, due to variable solar irradiance, it cannot produce constant power throughout the day.

There are mainly two kinds of photovoltaic systems: on-grid and standalone. In a standalone PV system, solar energy is converted into DC through PV array and stored in batteries. The stored energy in batteries is used to run the appliances. While in an on-grid system, DC power produced by PV is not used to charge the batteries; rather, it is converted into AC by the inverter and fed to the grid. Nowadays, grid-tied PV systems are gaining more attention than standalone systems as they can be integrated

S. K. Das (✉) · M. K. Sinha · A. K. Prasad
Mechanical Engineering Department, NIT Jamshedpur, Jamshedpur, Jharkhand, India
e-mail: shamikdeep96@gmail.com

M. K. Sinha
e-mail: mksinha.me@nitjsr.ac.in

A. K. Prasad
e-mail: akprasad.me@nitjsr.ac.in

O. H. Gupta et al. (eds.), *Recent advances in Power Systems*, Lecture Notes in Electrical Engineering 960, https://doi.org/10.1007/978-981-19-6605-7_13

with thermal and hydropower plants into hybrid power systems. The simplest on-grid system consists of a solar panel and an inverter unit [1] but we have introduced a boost converter in between the PV array and the inverter to level up the voltage output from the PV array, and an LCL filter is attached at the end of the inverter to die out the harmonics.

Due to the lower conversion efficiency (from solar energy to electrical energy) of PV, i.e., 9–15%, and variable solar irradiance, MPPT is a major portion of a grid-linked PV system to ensure that the highest power is always drawn out from the PV panel [2–5]. Various MPPT algorithms have been introduced in the literature. Among them, the most popular is the "P & O" method and the "Incremental Conductance" method [6–9]. A three-phase inverter is required for DC to AC power conversion. One-cycle control and conventional PWM are some of the strategies to control 3-phase inverters [10]. To adjust active and reactive power in single-stage photovoltaic structures, vector control and voltage and current double closed-loop controls can be used [11, 12]. To synchronize the grid voltage, we need to implement a Phase Lock Loop (PLL) using the Synchronous Reference Frame theory, which also shows the necessity of Clark and Park Transformation [13]. To die out the harmonics, the LCL filter is favored over the L-filter and LC-filter as it can come up with a lesser THD and improved decoupling between the filter and grid impedance [14]. We can tune the controller using classical Ziegler–Nichols, but only in a limited area [15]. In our study, the P&O algorithm has been implemented in MPPT control. In this paper, the dynamic performance of a two-stage, three-phase, grid-linked PV system under variable solar irradiance has been simulated in MATLAB/Simulink software. This study also shows the parameter calculations of the Boost converter and the LCL filter.

2 Schematic Layout of the Model

Figure 1 shows the schematic layout of the system.

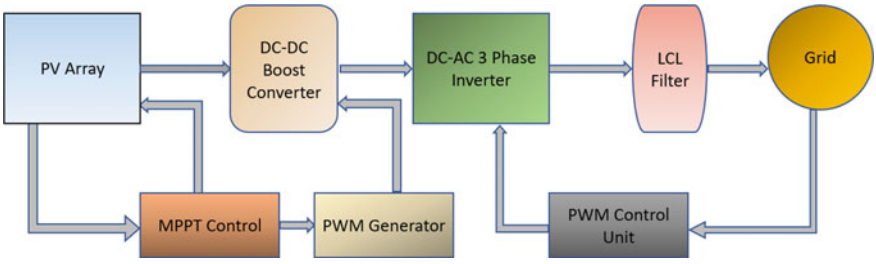

Fig. 1 Schematic figure of grid-linked PV system

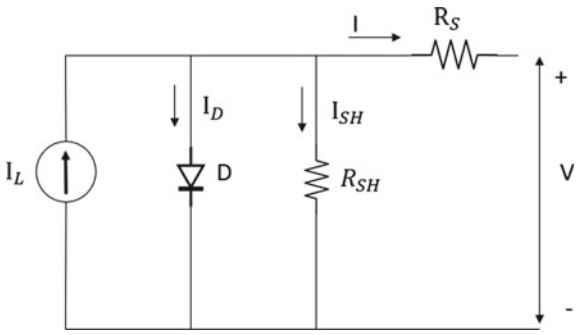

Fig. 2 Equivalent circuit figure of a PV Cell

3 System Components

The proposed model contains of the below units.

(a) PV Array, (b) Boost Converter, (c) MPPT Control, (d) 3-Phase Inverter, (e) LCL Filter, and (f) Power Grid.

4 PV Array

4.1 Working Principle

The conversion of light energy into electrical energy is known as the Photovoltaic Effect. A PV cell is made of semiconductor material. When Silicon is doped with Boron (pentavalent atom), it creates an *n*-type semiconductor and when it is doped with Phosphorus (trivalent atom), it forms a *p*-type semiconductor. These two types of semiconductors are sandwiched together to make a PV cell. When a photovoltaic cell is brought to sunlight and photon energy is higher than the bandgap energy of the *p*–*n* junction, generation of electron–hole pair takes place. The excited electrons flow to the *n*-side due to an electric field and holes sweep to the *p*-side. The free charges are collected from the electrical joints applied to either edge before passing to the outer circuit in the form of electricity. It gives rise to the direct current. The equivalent circuit figure of a solar cell has been shown in Figs. 2 and 3 represents the *I*-*V* characteristic of a PV cell. The OCC, SCC, and MPP have also been pointed to the below figure.

4.2 Equivalent Circuit and Current Equation

The output current from solar cell is given by Eq. (1)

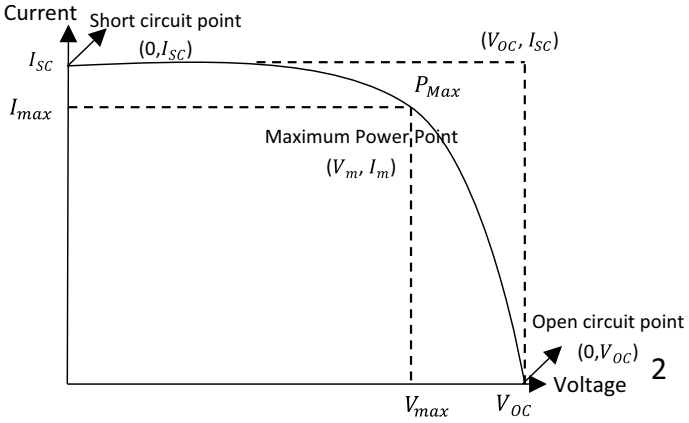

Fig. 3 *I-V* characteristics of solar cell

$$I = I_{\mathrm{L}} - I_{\mathrm{D}}\left(e^{\frac{q(V+IR_S)}{kT}} - 1\right) - \frac{V + IR_{\mathrm{S}}}{R_{\mathrm{SH}}} \tag{1}$$

I Cell output current (Amp)
I_{L} Photon generated current (Amp)
I_{D} Diode saturation current
q Charge of an electron $= 1.6 * 10^{-19}$ Coulombs
k Boltzmann constant
T Cell temperature (K)
R_{SH} Shunt resistance
R_{S} Series resistance
V Cell output voltage (Volt)

A PV array is several individual PV panels electrically connected whereas a PV panel is a collection of a single PV cells. We have taken 47 strings consisting of 10 PV modules connected in series with maximum power output from a single PV cell 213.15 W to produce 100 kW power (47 * 10 * 213.15 = 100.18 kW). We have shown the solar cell parameters value in Table 1 for the proposed model.

The *P-V* & *I-V* characteristics of the PV cell used in the proposed model is depicted in Fig. 4. For solar irradiance of 1 kW/sq-m, the maximum power generation by the PV Array is 100 kW.

5 Boost Converter

A fixed DC input voltage can be directly converted into a variable DC output voltage by using a chopper. In this model, we have used an IGBT as a power semiconductor

Table 1 Specification of solar cell

Solar cell data	Ratings
Maximum power (Watt)	213.152
Cells per module (N_{cell})	60
O/C voltage V_{oc} (Volt)	36.2
S/C current I_{sc} (Amp)	7.83
Voltage at MPP, V_{mpp} (Volt)	29.0
Current at MPP, I_{mpp} (Amp)	7.34
Temperature coefficient of V_{oc}(%/°C)	−0.36099
Temperature coefficient of I_{sc}(%/°C)	0.102

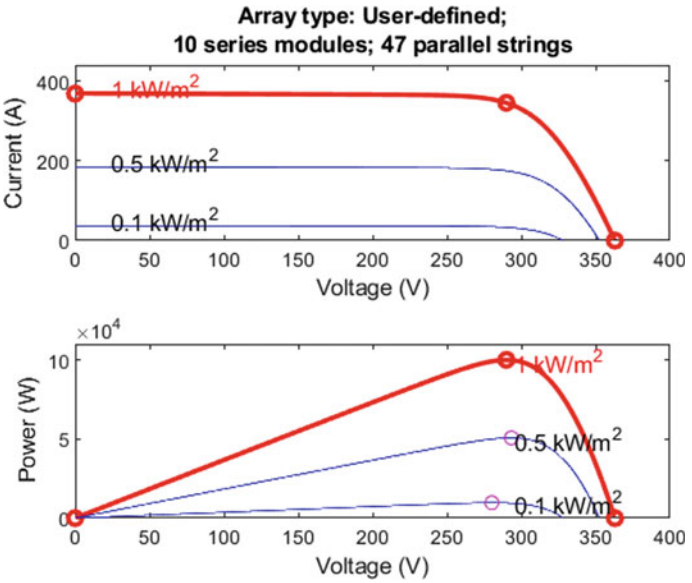

Fig. 4 *I-V* and *P-V* characteristic of the solar cell used in the proposed system

device for making the boost chopper circuit. The schematic circuit diagram of a Boost Chopper is shown in Fig. 5.

If we equate stored energy in the inductor for T_{on} and energy released by the inductor to the load during T_{off}, we will get the average output voltage as

Average output voltage, $V_{output} = \frac{V_{input}}{1-D}$, where D = duty ratio

Average output current, $I_{output} = I_{input}(1 - D)$

$$D = \frac{T_{on}}{T_{on} + T_{off}}$$

T_{on} On time duration of IGBT

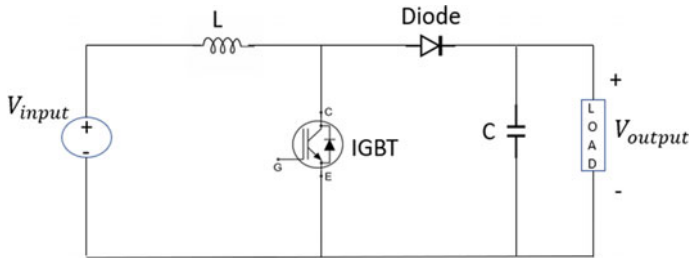

Fig. 5 Schematic figure of a boost chopper

T_{off} Off time of duration IGBT device

$$T_{\text{sw}} = T_{\text{on}} + T_{\text{off}}$$

Switching frequency, $f_{\text{sw}} = \frac{1}{T_{\text{sw}}}$.

6 MPPT Design

As a solar cell is a non-linear device, it is not able to produce constant power throughout the day due to its dependency on two important parameters, solar irradiance, and temperature. Temperature and solar irradiance depend on the atmospheric conditions and many other factors due to which they vary throughout the day and because of that the output power from the solar cells is not constant either. In the grid-linked PV model, we have to draw out the highest power from the solar cells for which we need an MPPT algorithm. The 'Perturb & Observe' algorithm is one of the best-suited methods which gives accurate results in maximum power point tracking. The flow chart of the Perturb & Observe algorithm is shown in Fig. 6 and the *P-V* characteristic of solar cells with MPP conditions has been shown in Fig. 7.

6.1 P&O Algorithm Flow Chart

As shown in Fig. 6, in the beginning, output voltage and current at any instance from PV are read. The Power $P = V * I$ is then calculated. After that the difference between the previous and present value of voltage and power is determined. Now observe whether the power has increased or reduced, i.e., $dP > 0$ or not. If YES, that means power has increased. Next check the condition $dV > 0$. If it is YES, that means we are moving in the correct direction. In the next step, increase the voltage

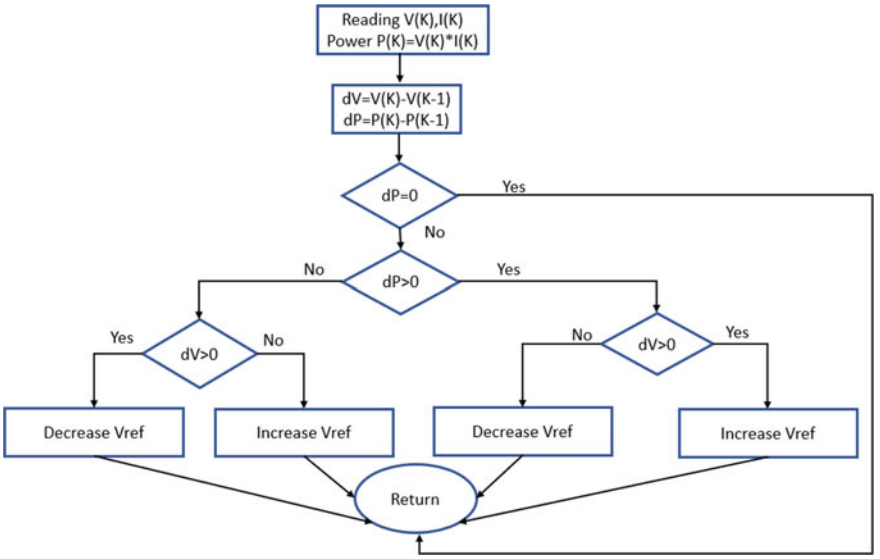

Fig. 6 Flow chart of P&O method for highest power point tracing

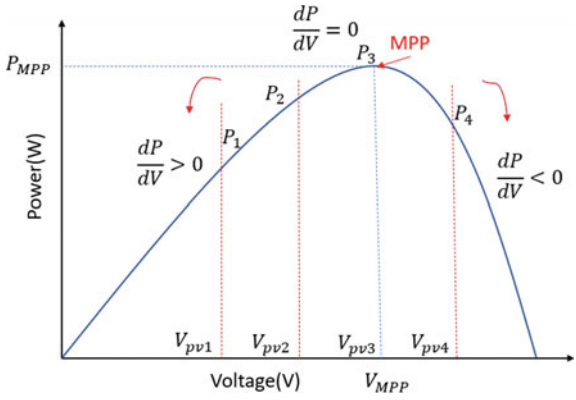

Fig. 7 *P-V* characteristic of a solar cell

and if the condition becomes false, decrease the voltage to obtain maximum power. In addition, if d$P < 0$ and d$V > 0$, lower the reference voltage to obtain MPP.

6.2 Maximum Power Point Tracking Using Boost Chopper

In Fig. 8 we have shown the schematic block diagram and control operation of the highest power point tracing using a boost chopper. The following steps show the control procedure.

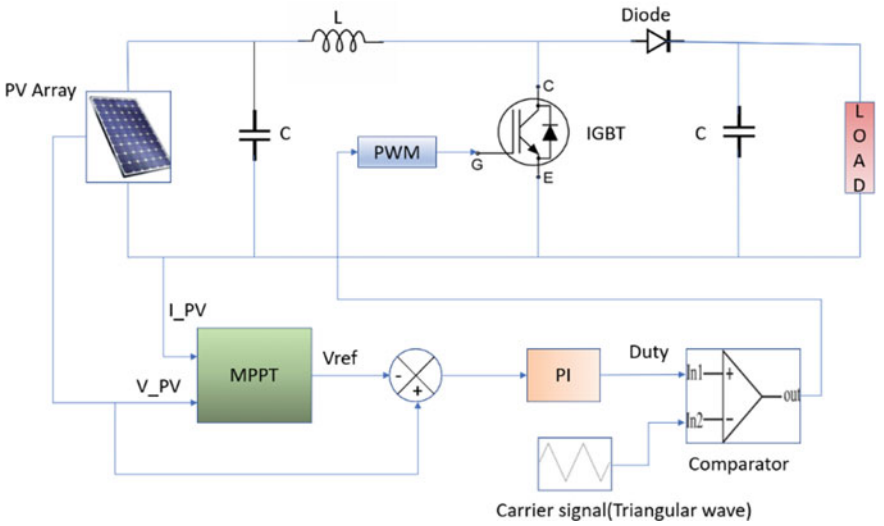

Fig. 8 Block diagram of highest power point tracing using boost chopper

- Sense the current I_PV voltage and V_PV from the solar panel.
- We get V_{ref} as output from the MPPT block.
- Actual PV voltage V_PV is tallied with MPPT output V_{ref} and the error value is applied to the PI controller.
- Triangular wave as a carrier signal is fed to the comparator and compared with PI controller output and the PWM is applied to Gate terminal of IGBT.

The MPPT MATLAB figure is shown in Fig. 9. The Boost converter has been connected to the output of the PV array. The voltage and current from the PV array are measured and the P&O algorithm is implemented in MATLAB Function. The generated PWM is then fed to IGBT to boost up the output voltage at the required level.

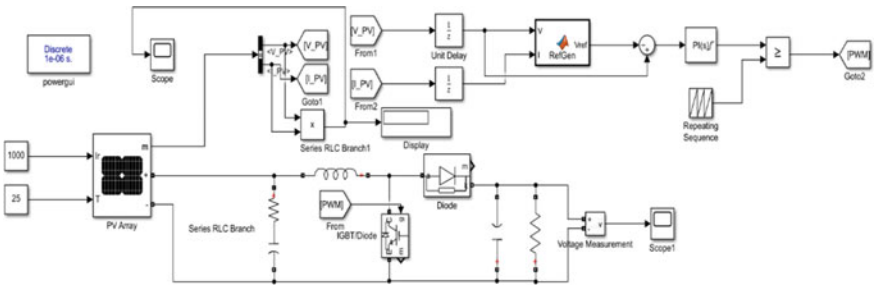

Fig. 9 MPPT implementation in MATLAB

7 Three-Phase Inverter

MATLAB implementation of a three-phase inverter has been shown in Fig. 10. PWM has been used as an internal control method for the inverter. By controlling the ON time and OFF time of IGBTs, we can obtain a controlled output voltage from a fixed DC voltage.

7.1 Synchronous Reference Frame Theory (SRF)

The SRF Theory has been incorporated to implement the control mechanism of a three-phase inverter. First, the three-phase voltage V_{abc} is measured by the 3-phase *V-I* Measurement block. Then V_{abc} is converted into a 2-Phase frame, i.e., an alpha–beta frame by using Clark's Transformation as shown in Eq. (2). V_α and V_β come as output after Park's Transformation as shown in Eq. (3). These two voltages are used to implement the Phase Lock Loop (PLL) from which we get ωt as output. V_α and V_β are then transformed into *d-q* frame voltages V_d and V_q with the help of Park's Transformation. The phasor diagram of *a-b-c* and alpha–beta frames has been shown in Fig. 11.

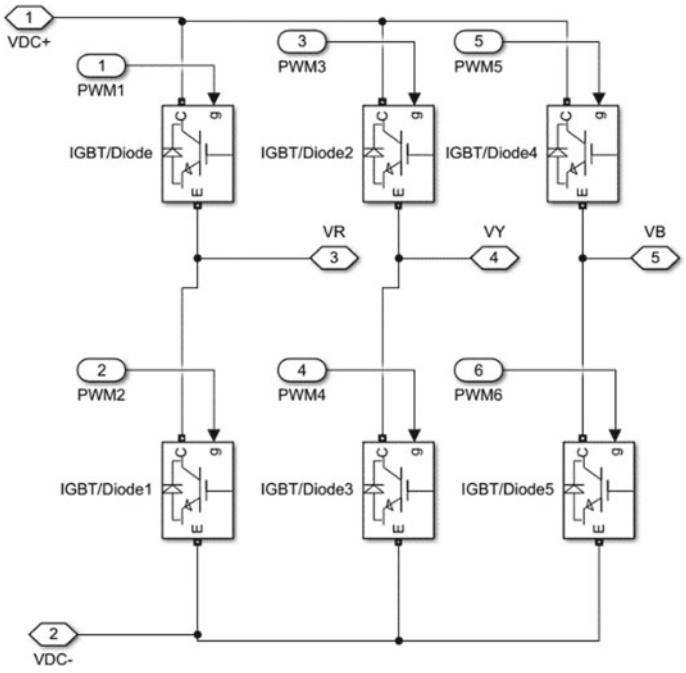

Fig. 10 Circuit design of a three-phase bridge inverter

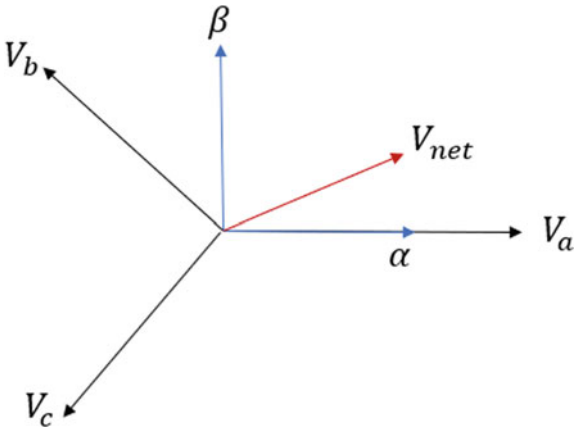

Fig. 11 Phasor diagram of *a-b-c* and alpha–beta frame

Clark's Transformation Matrix

$$\begin{bmatrix} x_\alpha \\ x_\beta \\ x_0 \end{bmatrix} = \frac{2}{3}\begin{bmatrix} 1 & -1/2 & -1/2 \\ 0 & \sqrt{3}/2 & -\sqrt{3}/2 \\ 1/2 & 1/2 & 1/2 \end{bmatrix}\begin{bmatrix} x_a \\ x_b \\ x_c \end{bmatrix} \tag{2}$$

Park's Transformation Matrix

$$\begin{bmatrix} x_d \\ x_q \\ x_0 \end{bmatrix} = \begin{bmatrix} \cos\theta & \sin\theta & 0 \\ -\sin\theta & \cos\theta & 0 \\ 0 & 0 & 1 \end{bmatrix}\begin{bmatrix} x_\alpha \\ x_\beta \\ x_0 \end{bmatrix} \tag{3}$$

As shown in Fig. 12, next, 3-phase inverter current I_{abc} is sensed and transformed into *d-q* frame current I_d and I_q after sequentially passing through Clark's Transformation and Park's Transformation. I_d and I_q are then compared with the reference current along the *d*-axis and *q*-axis and the differential value is applied to the PI controller, which causes the voltage signal in the *d-q* frame. These voltage signals are added with some gain and transformed into an *a-b-c* frame from a *d-q* frame by using Inverse Park's Transformation and Inverse Clark's Transformation. As a result, we get V_{abc_ref} which will be used to generate PWM for 3-phase Inverter.

Figure 13 shows the voltage and current transformation block which converts three-phase voltage and current into the *d-q* frame by performing Clark and Park transformation simultaneously.

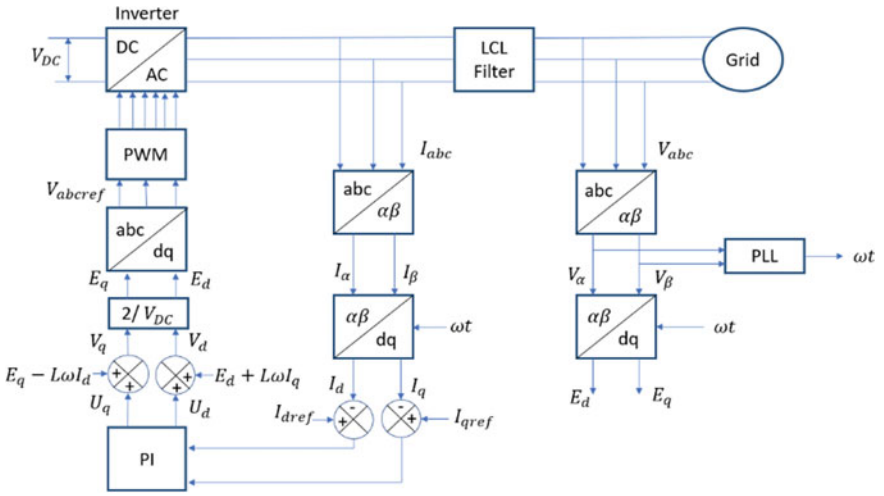

Fig. 12 Controller block diagram for the 3-phase grid-tied inverter

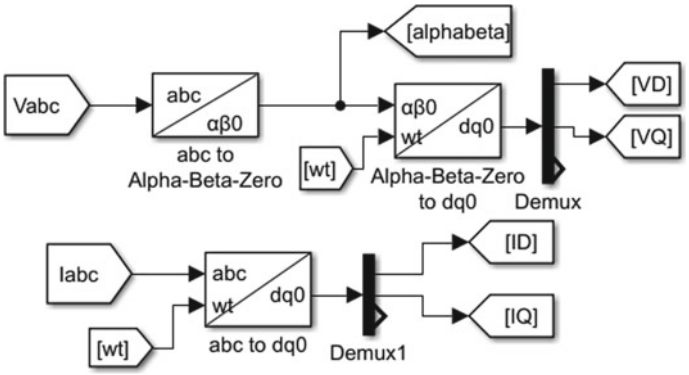

Fig. 13 Voltage and current transformation block

7.2 Phase Lock Loop (PLL)

The *d*-*q* frame is a rotating frame whose speed of rotation may or may not be equal to the speed of rotation of the grid voltage. To simplify the controller, we have to make the *d*-*q* frame stationary with respect to the grid voltage. Our aim is to lock or align the grid voltage vector along the *d*-axis and make the *q*-component of grid voltage zero. Suppose, we have a positive value of V_q and V_d. The net grid voltage V_{grid} is now not aligned with the *d*-axis. That means, the speed of the *d*-*q* frame is slower and we have to accelerate it so that the *d*-axis get aligned with the grid voltage. Figure 14 shows the alpha–beta and *d*-*q* frame where the V_{grid} is not aligned with the *d*-axis due to the presence of a voltage component along the *q*-axis. But grid voltage gets

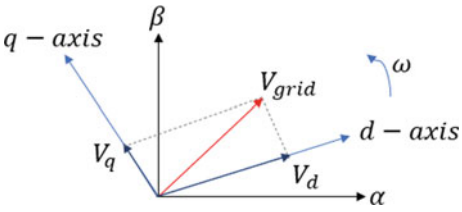

Fig. 14 Net grid voltage

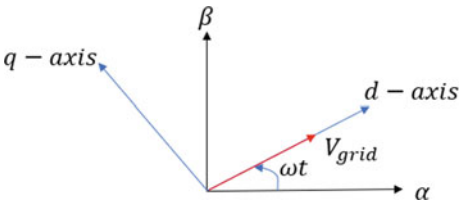

Fig. 15 Alignment of grid voltage with *d*-axis

aligned with *d*-axis when we apply PLL to modify the ωt value which is shown in Fig. 15.

Figure 16 shows the schematic diagram of the PLL controller. Three-phase voltages V_a, V_b and V_c are converted into V_d and V_q by using the transformation techniques shown above. The V_q component is compared with $V_{q_{\text{ref}}} = 0$. Next, the error value is fed to the PI controller which produces angular frequency ω. The ω is integrated to find out $\theta = \omega t$ and ωt is used as feedback to modify the voltage V_q.

Figure 17 shows the actual implementation of PLL in the Simulink environment.

The schematic diagram of the controller for grid-connected three-phase inverter in Fig. 12 has been constructed and executed in MATLAB/Simulink as depicted in Fig. 18. The controller has been developed to generate PWM pulses for the required operation of the inverter. The layout of the subsystem 'PWM' is depicted in Fig. 19.

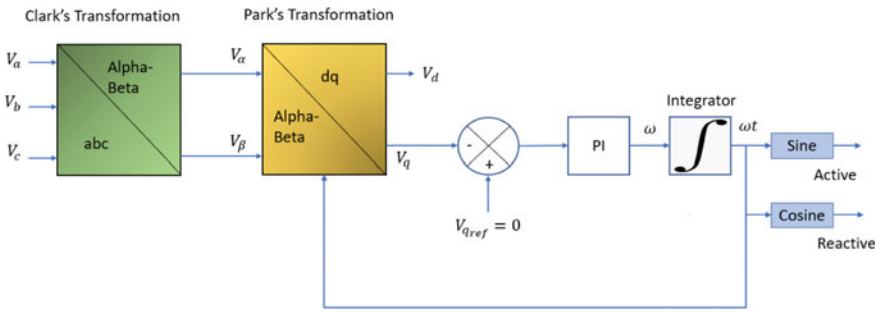

Fig. 16 The phase lock loop (PLL) controller block diagram

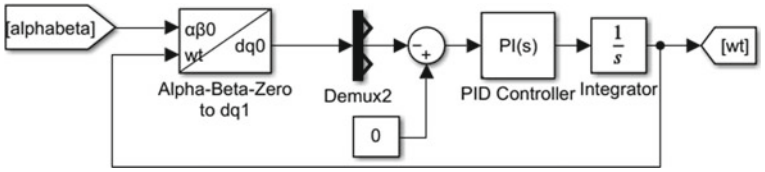

Fig. 17 Phase lock loop (PLL) implementation in MATLAB

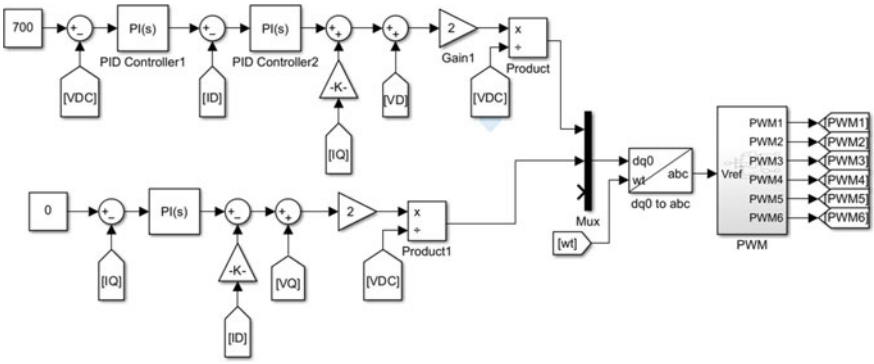

Fig. 18 Controller implementation of three-phase inverter in MATLAB/Simulink

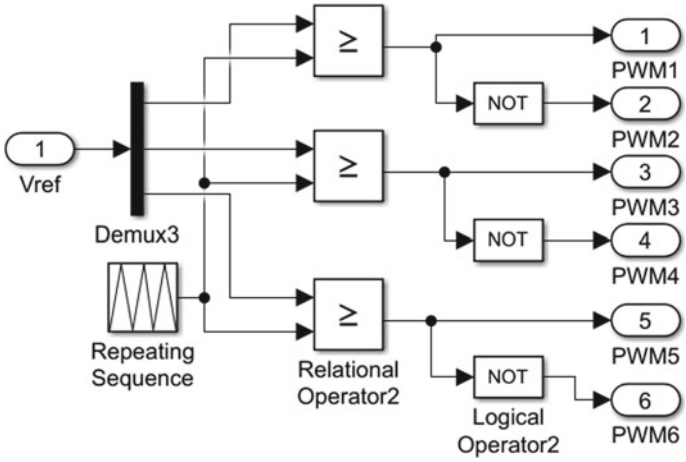

Fig. 19 PWM generation circuit diagram

8 LCL Filter

The output current from 3-phase inverter contents harmonics. Injection of this current into the grid may deteriorate voltage as well as power quality. To avoid these problems, we always connect a filter at the end of the inverter so that we can generate a smooth sinusoidal current before feeding into the grid. LCL filter is favored over L-filter and LC-filter as it can come up with a lesser THD and improved decoupling between the filter and grid impedance. That's why grid-linked employments mostly prefer LCL filters.

9 Power Grid

A Power grid is an electrically interconnected network among multiple generating stations to loads that supplies electricity to the consumers. An electrical grid consists of generating station to produce 3-phase AC power, an electrical substation to step up the voltage before feeding to a transmission line to reduce losses and transmission costs, transmission lines to transmit the power over long distances, and lastly the distribution system to distribute the 3-phase or single-phase AC power to commercial places and houses at required voltage level. Here we have considered Phase-to-Phase RMS voltage of grid is 400 V and frequency is 50 Hz.

10 Results and Discussion

10.1 Boost Converter Design

Specifications

Grid voltage = 400 V (RMS)

For the PV module, $V_{mpp} = 29$ V, as 10 modules are connected in series, the maximum output voltage from PV Array is 29 * 10 = 290 V

The minimum input voltage for inverter $= 400 * \sqrt{2} * 1.2 = 678.82$ V

The voltage output of Boost Chopper should be greater than the Inverter input voltage. Hence, we have considered $V_{output} = 700$ V for the Boost converter.

Specifications

$V_{input} = 290$ V, $V_{output} = 700$ V, Rated Power = 100 kW, Switching Frequency, f_{sw} = 5 kHz.

Calculation

Current Ripple, $\Delta I = 5\%$ of Input Current

Voltage Ripple, $\Delta V = 1\%$ of Output voltage

Input Current = 100 kW/290 V = 344.82 A

Current Ripple, $\Delta I = 5\%$ of 344.82 A = 17.24 A

Voltage Ripple, $\Delta V = 1\%$ of 700 V = 7 V

Output Current = 100 kW/700 = 142.85 A

In Boost Converter, $V_{\text{output}} = \frac{V_{\text{input}}}{1-D}$, where D = duty ratio

$$V_{\text{output}} = \frac{V_{\text{input}}}{1-D} \Rightarrow 700 = 290/(1-D) \Rightarrow D = 0.586$$

The peak-to-peak ripple current across the inductor is given by Eq. (4),

$$\Delta I = \frac{V_{\text{input}} D}{f_{\text{sw}} L} \tag{4}$$

From Eq. (4),

$$L = \frac{V_{\text{input}} D}{f_{\text{sw}} \Delta I} \tag{5}$$

$$\Rightarrow L = \frac{290 * 0.586}{5 * 10^3 * 17.24}$$

$$\Rightarrow L = 1.97\,\text{mH}$$

The peak-to-peak ripple voltage across the capacitor is given by Eq. (6),

$$\Delta V = \frac{I_{\text{output}} D}{f_{\text{sw}} C} \tag{6}$$

From Eq. (6),

$$C = \frac{I_{\text{output}} D}{f_{\text{sw}} \Delta V} \tag{7}$$

$$\Rightarrow C = \frac{142.85 * 0.586}{5 * 10^3 * 7} \Rightarrow C = 2391.71\,\mu\text{F}$$

10.2 LCL Filter Design

Switching Frequency, $f_{\text{sw}} = 10$ kHz

Resonant Frequency, $f_{\text{res}} = f_{\text{sw}}/10 = 10$ kHz/10 $= 1000$ Hz

Capacitance value depend on the reactive power required by the capacitor

Reactive Power, $Q = 5\%$ of Rated Power (S)

$$\begin{aligned} Q &= \frac{V_{\text{ph}}^2}{\frac{1}{2\pi f C}} = 5\% \text{ of } S \\ &\Rightarrow V_{\text{ph}}^2 * 2\pi f C = 0.05 * S \\ &\Rightarrow C = \frac{0.05 * S}{V_{\text{ph}}^2 * 2\pi f} \end{aligned} \tag{8}$$

For 100 KVA, 230 V_{p-p},50 Hz system, we calculate the capacitor value from Eq. (8)

$$C = \frac{0.05 * \left(100 * 10^3\right)/3}{230^2 * 2\pi * 50} = 100.28\,\mu F$$

The value of inductor L can be estimated by using Eq. (9),

$$L = \left| \frac{1}{w_{\text{sw}} * \frac{I_g(\text{sw})}{V_i(\text{sw})} * \left(1 - \frac{w_{\text{sw}}^2}{w_{\text{res}}^2}\right)} \right| \tag{9}$$

where

$w_{\text{sw}} = 2\pi\ f_{\text{sw}}$

$w_{\text{res}} = 2\pi\ f_{\text{res}}$

$V_g =$ Phase-to-phase Grid voltage

$I_g(\text{sw}) =$ Grid current at switching frequency

$V_i(\text{sw}) =$ Input voltage of LCL filter at grid frequency

For 100 KVA, 230 V_{p-p}, 50 Hz system

Grid Current, $I_g = (100$ KVA/3)/230 V $= 144.92$ A

$I_g(\text{sw}) = 0.3\%$ of $I_g = 0.003 * 144.92 = 0.434$ A

The minimum value of V_i at switching frequency is, $V_i(\text{sw}) = 0.9$ times $V_g = 0.9 * 230 = 207$ V

Table 2 Design parameters of boost converter and LCL filter

Parameters	Designed values
Boost converter switching frequency	5 kHz
Boost converter input voltage	290 V
Boost converter output voltage	700 V
Inductor (boost converter)	1.97 mH
Capacitor (boost converter)	2391.71 μF
Filter switching frequency	10 kHz
L(min)	76.68 μH
L(max) inverter side	500 μH
L(max) grid side	500 μH
Capacitor of LCL filter	100.28 μF
Rated power	100 kW

$$L = \left| \frac{1}{2\pi * 10000 * \frac{0.434}{207} * \left(1 - \frac{(2\pi * 10000)^2}{(2\pi * 1000)^2}\right)} \right| = 76.68\,\mu H$$

$L_1 = L_2 = L/2 = 38.84$ μH, is the minimum value of inductor.

The maximum value of the inductor is estimated based on the voltage drop across it.

Voltage drops across the inductor, $V_L = 20\%$ of V_g.

The maximum value of the inductor can be calculated by using Eq. (10)

$$L_{\max} = \frac{0.2 * V_g}{2\pi f I_g}$$
$$\Rightarrow L_{\max} = \frac{0.2 * 230}{2\pi * 50 * 144.92} = 1\,\text{mH} \tag{10}$$
$$L_1 = L_2 = L_{\max}/2 = 500\,\mu H$$

The design parameters of Boost Converter and LCL Filter are shown in Table 2.

10.3 Power Circuit Diagram

Figure 20 shows the power circuit model of the double stage Grid-Linked PV system which is designed in the MATLAB/Simulink environment.

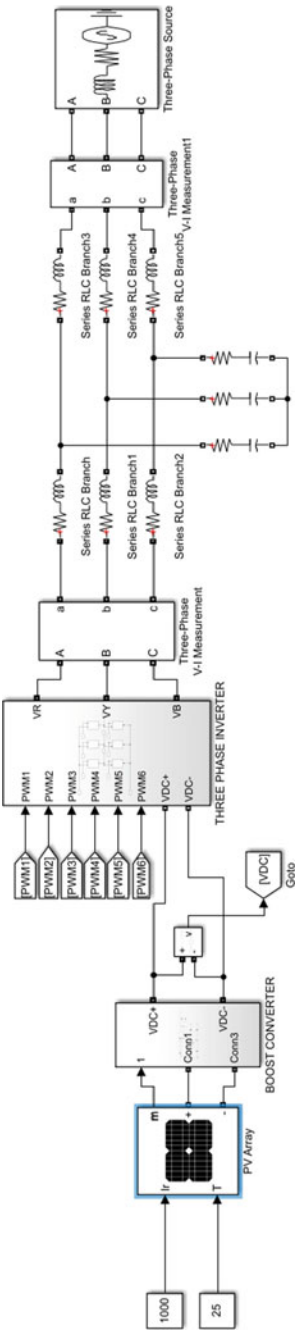

Fig. 20 Circuit diagram of double stage grid-linked PV model in MATLAB/Simulink

11 Simulation Results

11.1 The Output Power Graph from PV Panel

The Power output graph from PV Array at 1000 W/sq-m and 25 °C is 100 kW as shown in Fig. 21. The run time of the simulation is $t = 1$ s.

To visualize the dynamic behavior of grid-tied PV system we have varied the solar irradiance from 1000 W/sq-m to 100 W/sq-m the again increased it to 1000 W/sq-m for the time interval 0 to 1 s at 25 °C. As solar irradiance decreases gradually the output power from the PV array also reduce, but for a reduced irradiance also it will provide maximum power at that instance. Figure 22 shows the output power variation of the PV array due to varied irradiance. Figure 23 shows the output power variation of the PV array due to variation of temperature from 25 to 45 °C at constant solar irradiance of 1000 W/sq-m.

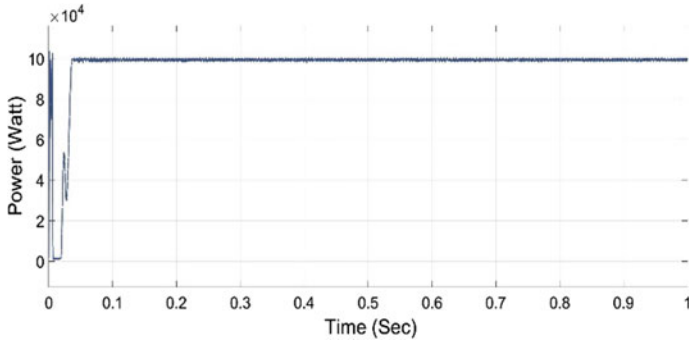

Fig. 21 Plot of power output from PV array

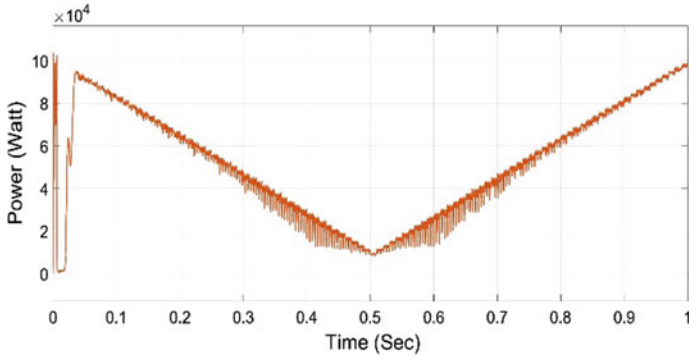

Fig. 22 Output power variation of PV for irradiance

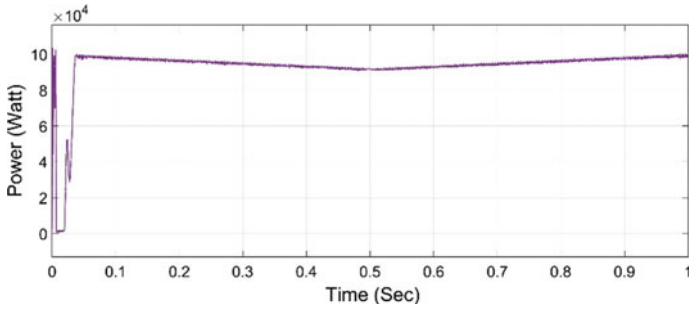

Fig. 23 Output power variation of PV array at variable temperature

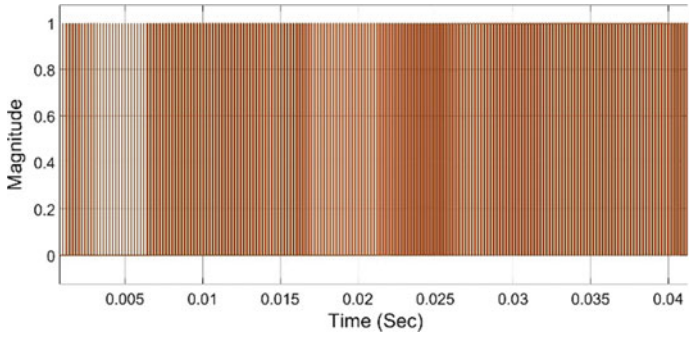

Fig. 24 PWM fed to IGBT in boost converter

11.2 Simulation Result from Boost Converter

Figure 24 shows the PWM pulses fed to IGBT in Boost Converter. A voltage measurement block has been connected at the end of Boost Chopper to read the DC output from the converter. Figure 25 shows the plot of DC output voltage Vdc from the converter. We are getting 700 V DC output which is fed to the inverter as an input voltage of the inverter.

11.3 Output Simulation Result

Figure 26 shows the PWM pulses which have been fed to the IGBT in three-phase inverter circuit. Here we have shown only four PWM pulses out of six.

Figures 27 and 28 show the plot of three-phase grid voltage and grid current. The phase-to-phase grid voltage is 400 V, 50 Hz. Phase to ground voltage can be calculated as $400 * \frac{\sqrt{2}}{\sqrt{3}} = 326.6$ V. The three-phase gird current decreases gradually

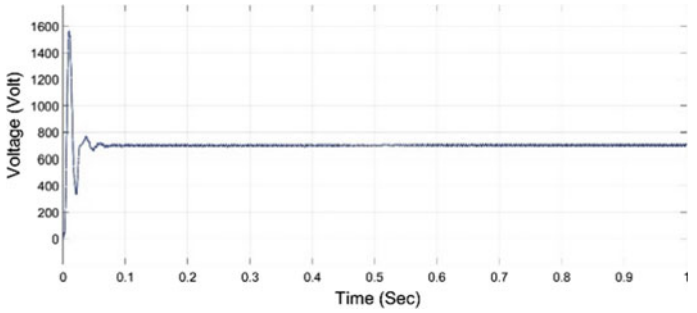

Fig. 25 DC output voltage from boost converter

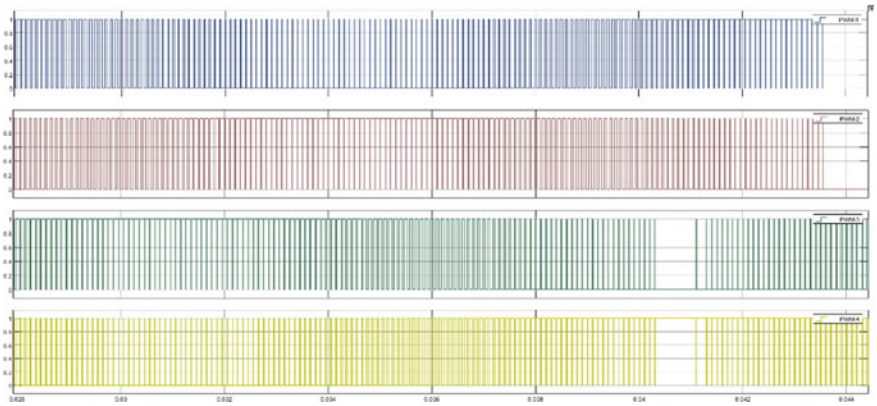

Fig. 26 PWM pulses for IGBT in three-phase inverter

from 0 to 0.5 s as the solar radiation varies from 1000 W/sq-m to 100 W/sq-m. Output current at $t = 1$ s is 200 A.

Figures 29 and 30 show the plot of grid voltage and grid current due to variation of temperature from 25 to 45 °C at constant solar radiation.

11.4 Simulation Result of Grid Power and Solar Radiation

Figures 31 and 32 show the variation of the grid power as the solar radiance is varying continuously. The output power is 100 kW at solar irradiance of 1000 W/sq-m. At $t = 0.5$ s the irradiance reduced to 100 W/sq-m and the corresponding output power also decreased to 1 kW. The first one is the plot of solar irradiance with time and the second one is the plot of output power.

The temperature has been varied from 25 to 45 °C at constant solar radiation which has been shown in Fig. 33 and the corresponding output power variation has

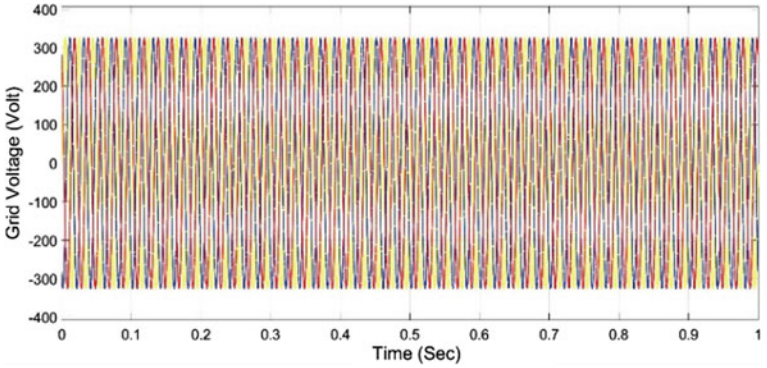

Fig. 27 Plot of grid voltage for variable irradiance

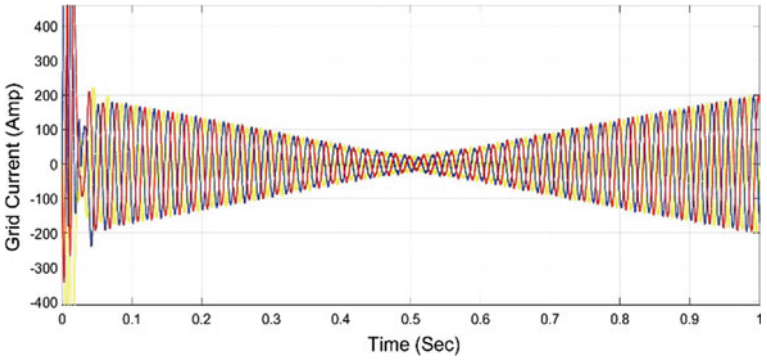

Fig. 28 Plot of grid current for variable irradiance

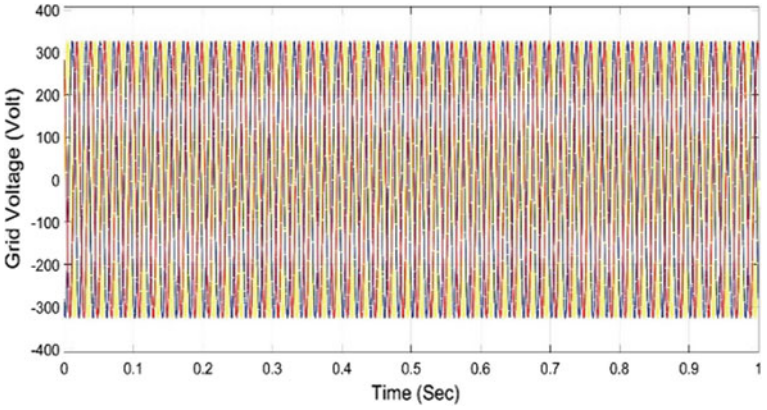

Fig. 29 Plot of grid voltage for variable temperature

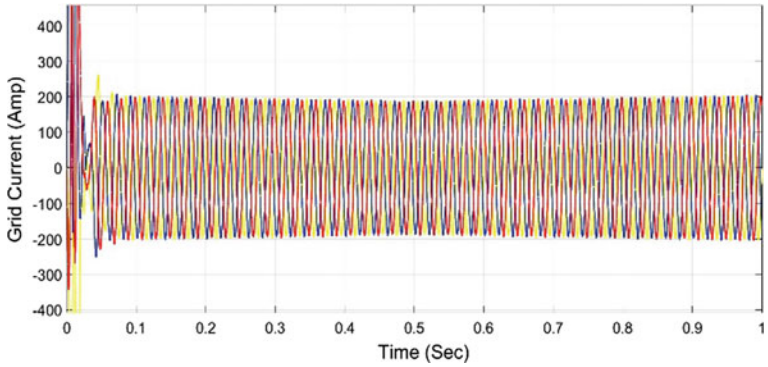

Fig. 30 Plot of grid current for variable temperature

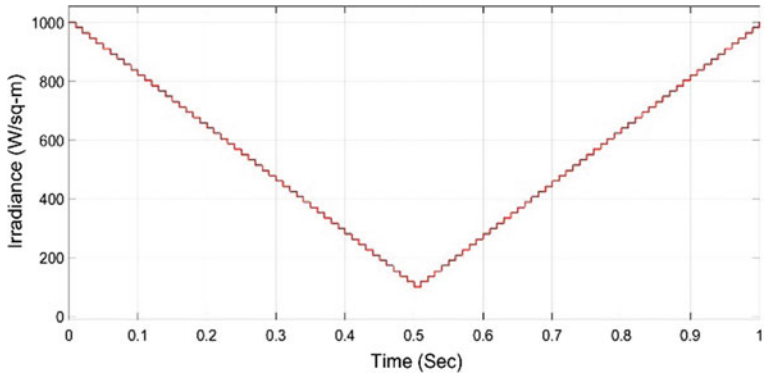

Fig. 31 Plot of solar irradiance versus time

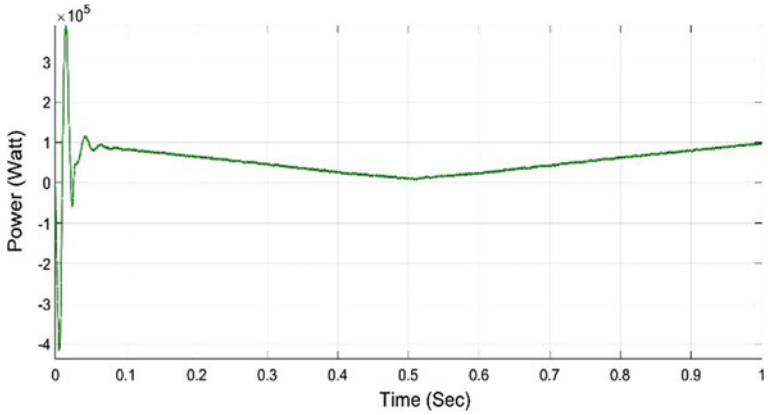

Fig. 32 Plot of output power versus time for irradiance

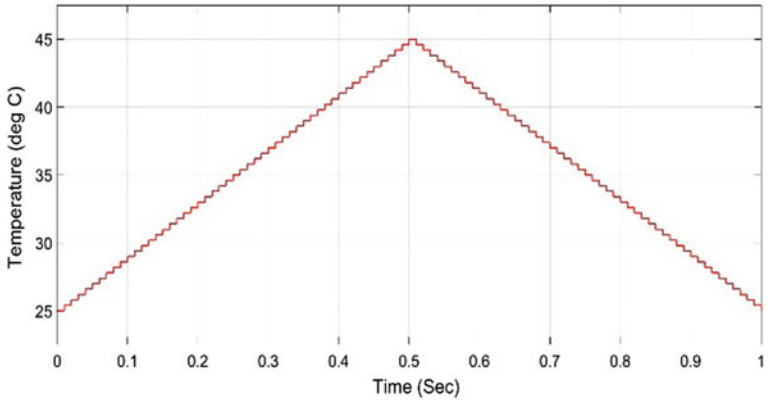

Fig. 33 Plot of temperature versus time

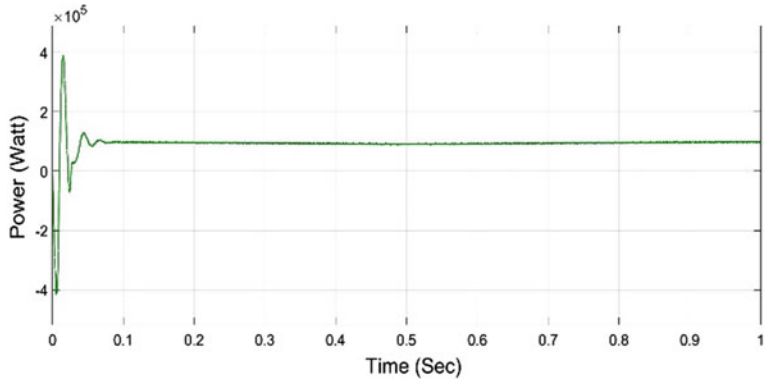

Fig. 34 Plot of output power versus time for temperature

been depicted in Fig. 34. MATLAB modeling of variable temperature and irradiance has been shown in Figs. 35 and 36. Real and reactive power has been displayed in Fig. 37.

12 Conclusion

In this paper, a Double Stage Grid-Linked PV System has been designed and simulated using MATLAB/Simulink version R2021a. The proposed system is able to generate 100 kW of power and feed it to the utility grid. The P&O method has been used in MPPT to draw out the highest power under variable circumstances. Inductance and capacitance values of boost converter have been calculated as 1.97 mH and 2391.71 μF, respectively. The DC output from the PV array is 290 V which is

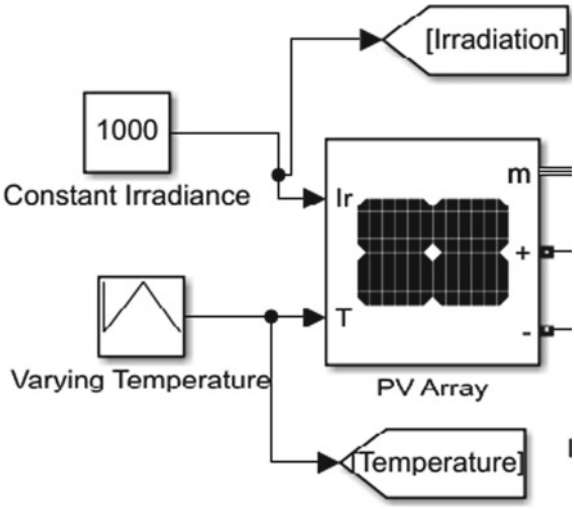

Fig. 35 Variable temperature at constant irradiance

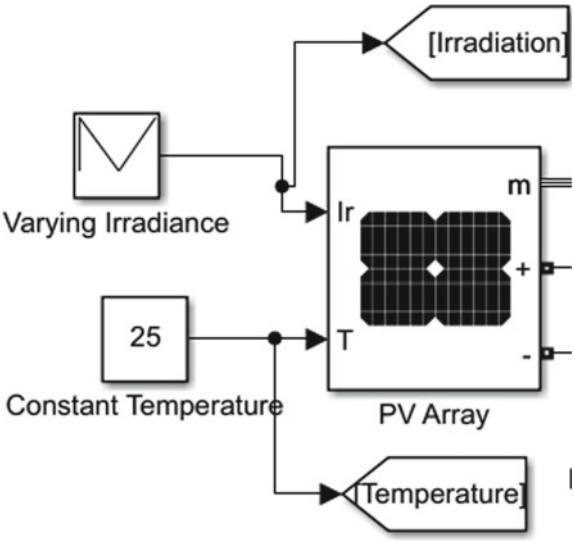

Fig. 36 Variable irradiance at constant temperature

boosted up to 700 V by the Boost converter and converted into AC by the 3-phase bridge inverter. Synchronous reference frame theory has been introduced to achieve PLL control. In LCL Filter the inductance value of 500 μH on the grid side as well as inverter side and the capacitance value of 100.28 μF have been estimated for particular specifications. The output of the inverter is passed through the LCL filter to remove the harmonic and maintain improved power quality of the grid. The solar irradiance has been varied from 1000 to 100 W/sq-m at a constant temperature of 25 °C and the plot of solar irradiance and real power output has been shown. A dip in

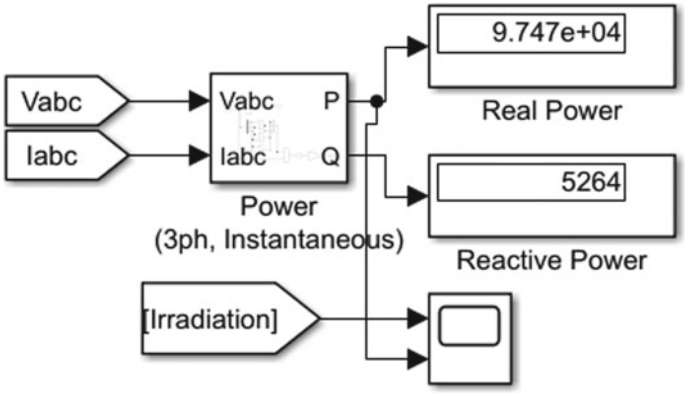

Fig. 37 Display of active and reactive power

real power is noticed due to a decrease in irradiance. The grid current drops drastically at 100 W/sq-m irradiance. Also, a slight dip in real power has been observed due to a change in temperature from 25 to 45 °C at constant solar radiation of 1000 W/sq-m. It has also been shown that the grid current remains almost constant with the temperature variation.

References

1. Jayaram, K.: Simulation based three phase single stage grid connected inverter using solar photovoltaics. J. Univ. Shanghai Sci. Technol. **23**(5) (2021)
2. Benaissa, O.M., Hadjeri, S., Zidi, S.A.: Modeling and simulation of grid connected PV generation system using Matlab/Simulink. Int. J. Power Electron. Drive Syst. (IJPEDS) **8**(1), 392–401 (2017)
3. Molina, M.G., Espejo, E.J.: Modeling and simulation of grid-connected photovoltaic energy conversion systems. Int. J. Hydrogen Energy (2013)
4. Sarath Chandrareddy, E., Chengaiah, Ch., Bullarao, D.: A 100 kw single stage grid-connected PV system with controlled DC-link voltage. Mater. Today Proc. (2020)
5. Ravalika, G., Suriyaprakash, M., Srinivas, D.: Grid related PV system with D-Statcom modelling and simulation. J. Resour. Manag. Technol. **11**(4), 374–381 (2020)
6. Kothari, D.P., et al.: Perturb and observe MPPT algorithm for solar PV systems-modeling and simulation. IEEE India Conference, 16–18 Dec 2011
7. El Hichami, N.: Maximum power point tracker method for grid connected photovoltaic system based on hill climbing technique. Turkish J. Comput. Math. Educ. **12**(11) (2021)
8. Shafeek, M.A., et al.: Modelling and simulation of DC-DC boost converter and inverter for PV system. Malays. J. Sci. Adv. Technol. (2021)
9. Kasera, J., Kumar, V., Joshi, R.R., Maherchandani, J.K.: Modelling and simulation of grid connected photovoltaic system employing Pertub and observe MPPT algorithm. In: International Conference on Recent Trends of Computer Technology in Academia (2012)
10. Chen, Y., Smedley, K.: Three-phase boost-type grid-connected inverter. IEEE Trans. Power Electron. **23**(5) (2008)
11. Fethi, A.: Power control of three phase single stage grid connected photovoltaic system. IEEE Trans (2016)

12. Wu. X., Xu, F.: Control and simulation on three-phase single-stage photovoltaic (PV) system as connecting with power grids. In: IEEE Workshop on Electronics, Computer and Applications (2014)
13. Aillane, A., Chouder, A., Dahech, K.: P/Q control of grid-connected inverters. In: 18th International Multi-Conference on Systems, Signals & Devices (SSD'21) (2021)
14. Lettl, J., Bauer, J., Linhart, L.: Comparison of different filter types for grid connected inverter. In: PIERS Proceedings, Marrakesh, MOROCCO, 20–23 March 2011
15. Deželak, K., et al.: Proportional-integral controllers performance of a grid-connected solar PV system with particle swarm optimization and Ziegler–Nichols tuning method. Energies2021 (2021)